



# At-line bioprocess monitoring by immunoassay with rotationally controlled serial siphoning and integrated supercritical angle fluorescence optics



Charles E. Nwankire<sup>a,c,\*</sup>, Gerard G. Donohoe<sup>a,b,1</sup>, Xin Zhang<sup>a,b</sup>, Jonathan Siegrist<sup>a,c</sup>, Martin Somers<sup>a</sup>, Dirk Kurzbuch<sup>a,c</sup>, Ruairi Monaghan<sup>a</sup>, Maria Kitsara<sup>c</sup>, Robert Burger<sup>a,c</sup>, Stephen Hearty<sup>a,b</sup>, Julie Murrell<sup>d</sup>, Christopher Martin<sup>d</sup>, Martha Rook<sup>d</sup>, Louise Barrett<sup>a</sup>, Stephen Daniels<sup>a,e</sup>, Colette McDonagh<sup>a,c</sup>, Richard O'Kennedy<sup>a,b</sup>, Jens Ducreé<sup>a,c</sup>

<sup>a</sup> Biomedical Diagnostics Institute, National Centre for Sensor Research, Dublin City University, Glasnevin, Dublin 9, Ireland

<sup>b</sup> School of Biotechnology, Dublin City University, Glasnevin, Dublin 9, Ireland

<sup>c</sup> School of Physical Sciences, Dublin City University, Glasnevin, Dublin 9, Ireland

<sup>d</sup> EMD Millipore Corporation, 80 Ashby Road, Bedford, MA, USA

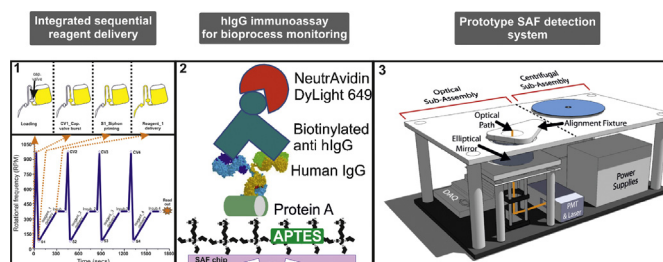
<sup>e</sup> National Centre for Plasma Science Technology, Dublin City University, Glasnevin, Dublin 9, Ireland

## HIGHLIGHTS

- Sample-to-answer microfluidic lab-on-a-disc device for at-line bioprocess monitoring.
- Centrifugally integrated and automated reagent delivery by serial-siphon valves.
- Supercritical angle fluorescence optics embedded on centrifugal platform.
- Development of fluorescence-linked-immunosorbent assay on human immunoglobulin G.
- Bioprocess samples from industrial reactor determined on the prototype system.

## GRAPHICAL ABSTRACT

A serial siphon based centrifugal microfluidic platform for the quantitative at-line monitoring of human immunoglobulin G (hIgG) in typical industrial bioprocess samples using a prototype optical SAF detection system.



## ARTICLE INFO

### Article history:

Received 14 December 2012

Received in revised form 28 February 2013

Accepted 8 April 2013

Available online 18 April 2013

### Keywords:

Lab-on-a-disc

Microfluidics

Bioprocess monitoring

Supercritical angle fluorescence

Integrated

## ABSTRACT

In this paper we report a centrifugal microfluidic “lab-on-a-disc” system for at-line monitoring of human immunoglobulin G (hIgG) in a typical bioprocess environment. The novelty of this device is the combination of a heterogeneous sandwich immunoassay on a serial siphon-enabled microfluidic disc with automated sequential reagent delivery and surface-confined supercritical angle fluorescence (SAF)-based detection. The device, which is compact, easy-to-use and inexpensive, enables rapid detection of hIgG from a bioprocess sample. This was achieved with, an injection moulded SAF lens that was functionalized with aminopropyltriethoxysilane (APTES) using plasma enhanced chemical vapour deposition (PECVD) for the immobilization of protein A, and a hybrid integration with a microfluidic disc substrate. Advanced flow control, including the time-sequenced release of on-board liquid reagents, was implemented by serial siphoning with ancillary capillary stops. The concentration of surfactant in each assay reagent was optimized to ensure proper functioning of the siphon-based flow control. The entire automated

\* Corresponding author at: Dublin City University, Biomedical Diagnostics Institute, Glasnevin, Dublin 9, Dublin, Ireland. Tel.: +353 873263676.

E-mail address: [charles.nwankire@dcu.ie](mailto:charles.nwankire@dcu.ie) (C.E. Nwankire).

<sup>1</sup> These authors contributed equally to this work.

microfluidic assay process is completed in less than 30 min. The developed prototype system was used to accurately measure industrial bioprocess samples that contained  $10 \text{ mg mL}^{-1}$  of hIgG.

© 2013 Elsevier B.V. All rights reserved.

## 1. Introduction

Microfluidic lab-on-a-chip [1] and in particular centrifugal lab-on-a-disc systems, continue to be a source of interest in both academia and industry, as they have a high potential to integrate laborious biochemical assay procedures onto a single, automated device with a small footprint and low cost [2–4]. While the emphasis of centrifugal microfluidic sample-to-answer systems is predominantly on clinical diagnostics, the monitoring of bioproduction processes is also an important area that remains relatively unexplored [5,6]. In bioprocess monitoring where product yield is of utmost economic importance, cells are engineered to produce recombinant proteins such as therapeutic antibodies [7]. The monitoring of cells and their products within a complex bioprocess matrix remains an important, demanding, expensive, difficult and challenging task [8]. Analytical techniques such as the use of Raman spectroscopy [6] and biosensors [9] have previously been explored for at-line bioprocess monitoring. However, issues such as sensor failure due to biofouling, inactivation of the sensing probe or non-specific binding have proven to be major obstacles [8]. As with clinical diagnostics, having a rapid, accurate, and easy-to-use test available at the point of sample collection would have tremendous benefit. Thus, the development of an ‘at-line’, ‘sample-to-answer’ microfluidic-based assay system for bioprocess monitoring is an important development for the bioprocess industry.

Although the design and fabrication of microfluidic chips is becoming more widespread, the modular integration of these chips with hardware systems, especially signal detection systems, remains a major engineering challenge [3,10–12].

For the first time, we present here a new system for the quantitation and monitoring of human immunoglobulin G (hIgG) by uniquely integrating a number of different technologies, namely—fluidic (centrifugal microfluidics) [13], immunoassay, optical (supercritical angle fluorescence) [10], and chemical (plasma enhanced chemical vapour deposition) [14] elements. Although these technologies (i.e. serial siphon valving [13], hIgG immunoassay [15], SAF collection technique [10] and APTES-functionalized Zeonor® [14,16]) have been reported separately; we for the first time demonstrate their integration for the fully automated quantification of hIgG in typical bioprocess samples.

In this work, we first outline the operational principle of the centrifugal, serial siphon controlled platform. Next, the custom benchtop hardware system for SAF detection is highlighted. Finally, the hIgG immunoassays performed on the opto-fluidically integrated lab-on-a-disc platform and the read-out on our custom-built benchtop SAF instrument are presented.

## 2. Operational principle

### 2.1. Centrifugal flow control by serial siphoning

Centrifugal microfluidic platforms have significantly advanced over recent decades. A variety of laboratory unit operations (LUOs) have been demonstrated on lab-on-a-disc technology, that includes: valving, metering, mixing, dilution, and particle handling [2,17,18]. Furthermore, centrifugal microfluidics has been shown to improve ‘flow-through’ assays, especially for surface-based assays, by decreasing total assay time, while producing results comparable to standard instrumentation but with increased assay sensitivity [2,19,20]. Fig. 1I shows the exploded assembly drawing of the

multi-layered, centrifugal “lab-on-a-disc” platform used in this work which will be outlined later in Section 3.1; a quarter segment of the disc with the microfluidic layout is represented in Fig. 1II. Fig. 1III illustrates a cross-sectional view of the fluidic flow over the assay spot through a micro-structured 3D via, and Fig. 1IV shows the several components of the hIgG sandwich immunoassay.

A common valving mechanism on centrifugal platforms is siphoning [13,17,21,22] where a liquid reservoir is connected to a hydrophilic outlet. This siphon channel starts at the outer end of this reservoir and bends inwards towards a crest point which is located closer to the centre of rotation than the (original) liquid level in the reservoir. Due to the hydrostatic equilibrium, the difference in filling levels of the reservoir and the inbound (“rising”) segment of the siphon diminishes at sufficiently high spin rates. Yet, when the spinning is slowed down, capillary action takes over to drive the liquid meniscus past the crest point and below the liquid level in the reservoir. At this stage, centrifugation leads to a depletion of the reservoir (Fig. 2A).

Unique to centrifugal platforms, siphoning can be used to stop flow at elevated spin rates and facilitate capillary flow, i.e. open the “gate”, at reduced pressures (i.e. low spin rates). No external, physical actuation mechanism (e.g., heating for wax melting) is required for the valves to function. Another advantage of siphon-based valving, is its tolerance to small spin-speed variations.

However, a particular challenge on centrifugal platforms is the implementation of the rotationally controlled, sequential release of multiple on-board liquids (i.e. sample and reagents). This problem was solved by placing a series of siphons next to each reagent reservoir. The number of windings in these serial siphons establishes the order of release in the assay. By using a series of cycles with slow and fast spinning rates, the reagents were consecutively released into a common flow (i.e. assay) channel. A fully assembled disc showing the serial siphons and the loading ports for the assay reagents is given in Fig. 1II.

In order to prevent capillary action from driving the liquid menisci through all the subsequent siphons, a (low pressure threshold) capillary stop, represented by a sudden geometrical expansion, was introduced in the inbound segment of each hydrophilic siphon channel (Fig. 2A).

After loading all liquids into their respective reservoirs at rest, the liquids protrude into their respective siphon outlets until they reach the (first) expansion. The spin rate is then increased to burst this first tier of capillary stops and thus let both the liquid levels in the reservoir and the rising parts of the outlet equilibrate. The disc is then decelerated until capillary action takes the menisci past their crest points and down the falling flanks. The liquids then either run against the next capillary stop at the entry of the subsequent siphon or they are released into the common outlet (Fig. 2A).

### 2.2. Supercritical angle fluorescence (SAF)

Amongst the many assay detection methods available, fluorescence-based methods provide sensitive and specific detection while not requiring physical contact with the device [12], which is an advantage for the rotational lab-on-a-disc platform. The chip comprises a focussing lens for excitation with a laser beam at 635 nm and a spherical ring lens structure at the bottom. The SAF emission is transmitted through the spherical structures at the bottom of the chip, thus avoiding total internal reflection (TIR) and is redirected by an elliptical mirror towards a

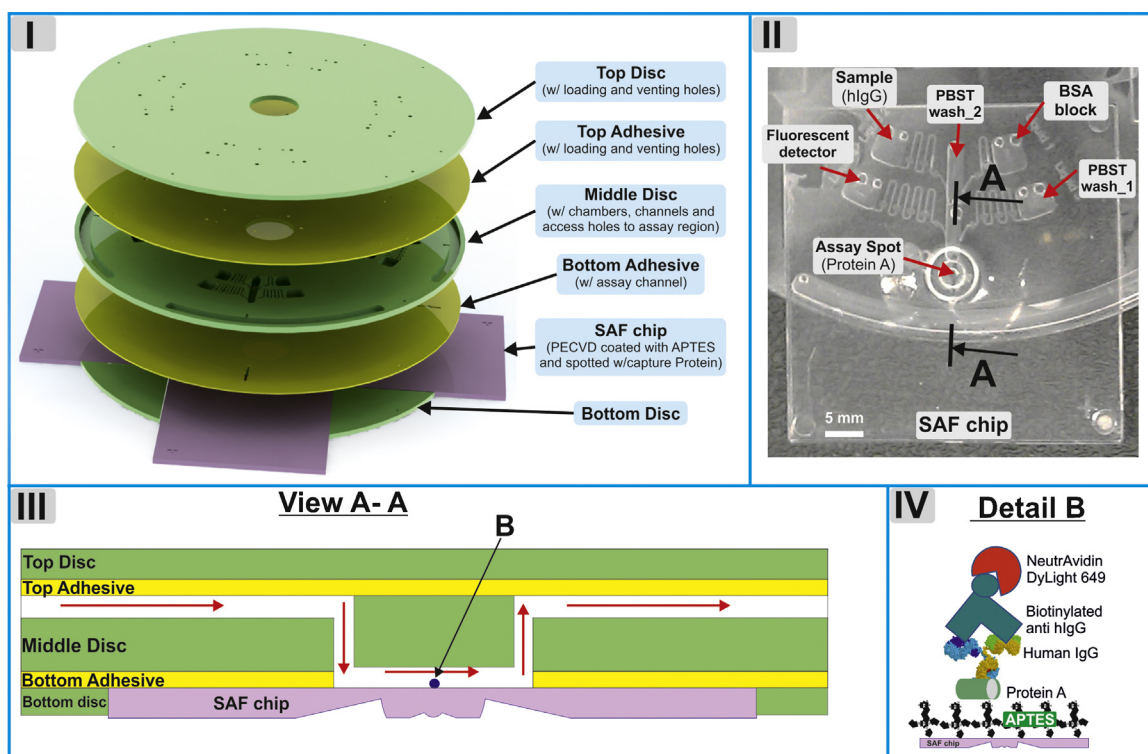


**Fig. 1.** (I) Exploded view of the disc showing the different layers made from acrylic (discs), adhesives and Zeonor (SAF chip). (II) Quadrant of the assembled microfluidic disc platform (top view) featuring the loading ports of the five FLISA reagents, with a section view (A–A) through the assay spot and SAF chip. (III) Cross-sectional view (A–A) of the 3D architecture of the microfluidic system network guiding the sample and reagents past the assay spot B (not drawn to scale). (IV) Schematic of the hIgG sandwich immunoassay (not drawn to scale). The SAF chips were PECVD-treated with APTES, and protein A was physically adsorbed onto the chip surface before assembly.

detector (Fig. 3A). The optical SAF setup very selectively collects the surface-specific fluorescence emanating from surface-bound emitters [10,23]. Compared to conventional fluorescence detection setups, our SAF scheme allows for a simpler and cost-efficient hardware system, which is suitable for hIgG detection.

In order to facilitate the immobilization of the capture biomolecule–protein A, plasma enhanced chemical vapour deposition (PECVD) technique was used to functionalize the SAF lens surface with aminopropyltriethoxysilane (APTES) [24,25].

### 3. Materials and methods

In this section, a description of the system component materials and fabrication methods is given. The prototype system consists of several components and sub-assemblies.

#### 3.1. Disc fabrication

The microstructured disc was designed using the CAD software package Pro/Engineer (PTC, US) and consisted of laminated layers of laser-cut and micro-milled polymethylmethacrylate (PMMA) (Radionics, Ireland), knife-cut pressure-sensitive adhesive (PSA) (Adhesives Research, Ireland), and injection-moulded Zeonor® 1060R (Zeon, JP) SAF chips (Protomold, UK) based on a preceding patent application [23] (Fig. 1II). The precision micro-milled siphon channels exhibit a cross section of  $250\ \mu\text{m} \times 250\ \mu\text{m}$ . The dimensions of the capillary valves are  $300\ \mu\text{m} \times 800\ \mu\text{m}$ . (Additional information related to the geometry and radial position of the siphon channels and capillary valves on the disc can be found in the ESI<sup>1</sup>.) The microchannel cut in the bottom adhesive was

specially designed to facilitate 3D fluidic flow over the assay spot on the SAF chip (Fig. 1III), and also to ensure that there were no liquid leakages. The bottom disc was custom designed and fabricated to facilitate the alignment of the centre of the SAF chip with the assay spot. The six different layers (top disc, top adhesive, middle disc, bottom adhesive, bottom disc and SAF chip) of the centrifugal microfluidic disc are shown in Fig. 1I; the discs were assembled using standard methods, with the help of an “in-house” engineered alignment jig [13,26].

#### 3.2. Surface chemistry and biomolecule immobilization

Cyclic olefin copolymers such as Zeonor® have the advantage of high optical clarity, low autofluorescence and the amenability to injection moulding, making them suitable for opto-microfluidic applications. However, due to the inertness of Zeonor®, it is extremely difficult to immobilise biomolecules on this polymer without prior surface modification [14,27]. To overcome this limitation, we utilized APTES to enable surface immobilization. Xiang et al. [27] established that chemical vapour deposition (CVD) produces a more homogeneous and denser coating, in comparison to liquid phase deposition of APTES. Extensive characterization of this APTES functionalized Zeonor® surface has previously been reported [14,16].

The SAF chips (Fig. 1II) were ultrasonically cleaned in surfactant, DI water and isopropanol, and then functionalized for biomolecule linking with APTES using the PECVD technique. An Oxford Plasmalab System100 PECVD reactor was used to carry out the deposition experiments. The process chamber was configured as a capacitively coupled system with an operating frequency of 13.56 MHz. Gas and precursor vapours were distributed uniformly throughout the chamber using a combination of an electrically isolated gas spreader and an RF powered shower head. During

<sup>1</sup> Electronic Supplementary Information (ESI) available.

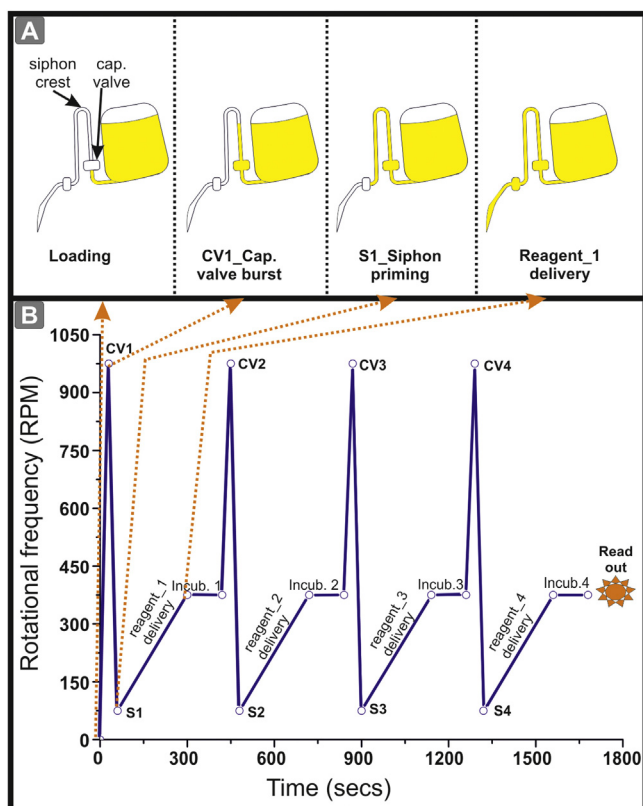


**Fig. 2.** (A) Schematic of a single cycle of the serial siphoning, from sample loading to reagent delivery; (B) Time curve of the rotational frequencies for the four serial siphon inline capillary burst valves (CV1–CV4)–975 RPM, siphon priming (S1–S4)–75 RPM, assay reagents (1–4) delivery–375 RPM, incubation (1–3)–375 RPM and read-out.

depositions, substrates were placed on a quartz holder, which was loaded onto the electrically grounded lower electrode of the plasma chamber, directly below the plasma shower head.

The chamber was maintained at a pressure of 200 mTorr during all process phases. Prior to deposition, plasma pre-treatment was performed to oxidise the substrate, using a mixture of argon and oxygen, and input power was set to 150 W for 3 min. After this pre-treatment, oxygen flow was stopped; the process power was

reduced to 5 W, and then APTES precursor vapour was introduced to the chamber. The liquid APTES precursor was supplied to the chamber through a heated stainless steel canister. There was a tendency of the APTES vapour to polymerize between the canister and chamber due to the thermal contours within the gas lines. In order to suppress this condensation which could lead to blockages or loss of flow to the chamber, the lines used were also maintained at an elevated temperature.

Amino-functionalization of the surface was carried out by plasma enhanced polymerization of APTES on the SAF chips. Subsequently, 100  $\mu\text{L}$  of Protein A (Piercenet, USA) (Fig. 1IV) at a concentration of 10  $\mu\text{g mL}^{-1}$  was directly coated by physical adsorption onto the chip surface. The SAF chips were incubated at 4 °C overnight. Thereafter, the chips were blocked for 1 h at 37 °C with a 1%, v/v solution of ‘hIgG-free’ bovine serum albumin (BSA) (Jackson ImmunoResearch Laboratories, USA).

All other polymer microfluidic components were ultrasonically cleaned before assembly.

### 3.3. Hardware instrument and microfluidic platform tests

The custom-engineered benchtop instrument consisted of 3D-printed polymer components (*inset* Fig. 3A). The instrument included a brushless motor for centrifugal spinning (Faulhaber, Germany) along with a spin-chuck to attach the microfluidic disc to the motor shaft. Control of the motor was enabled using a custom LabVIEW program (National Instruments, US) interfaced with a data acquisition system (National Instruments, US); a pre-set spinning protocol was programmed to establish a designated sequence of siphon priming and sample ‘flow-through’ to run the immunoassay. The development and optimization of the centrifugal microfluidic platform was performed on a standard centrifugal test stand, which was described previously [15,28]. The test stand comprises of a computer-controlled motor, a camera and a stroboscopic light for imaging a chosen area on the disc during rotation.

The detection system, designed “in-house”, consisted of a photo-multiplier tube (PMT) (Hamamatsu, Japan) for detection, a 635-nm, 5-nW laser diode (Hitachi, Ireland) for excitation, and various optical elements such as pinholes and lenses for collimation and focusing (ThorsLabs, USA). Control of the laser and PMT was enabled through the same LabVIEW program and hardware, as described above. The entire system was controlled via a data acquisition (DAQ) card that was connected to a standard laptop computer. A

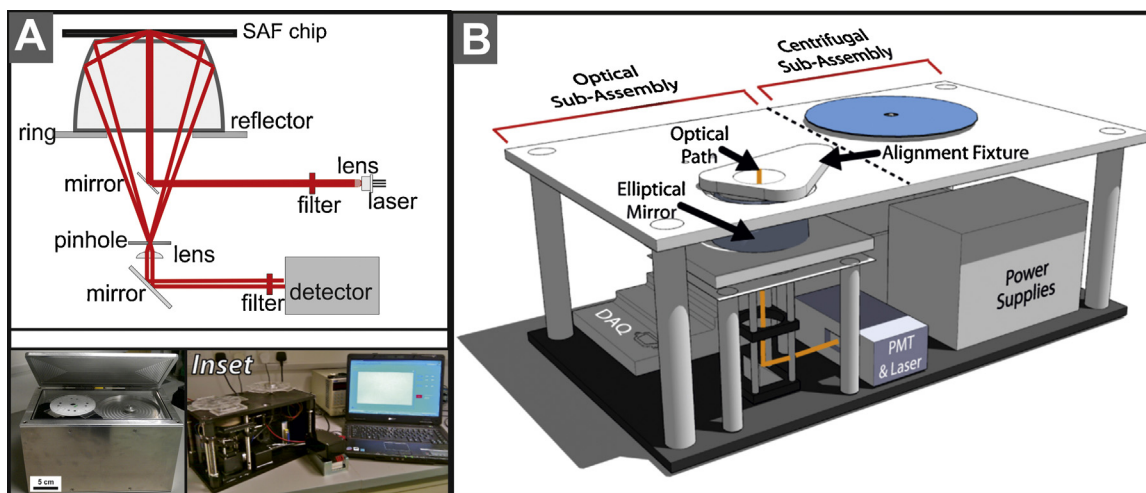


**Fig. 3.** (A) Optical paths of the SAF detection principle showing the collection of supercritical angle emission using the novel SAF chip. *Inset*: photo of the prototype system (with and without the housing unit) including laptop for control and the centrifugal microfluidic platform. The entire system measures approximately 18 cm  $\times$  18 cm  $\times$  33 cm (H  $\times$  W  $\times$  L); (B) 3D rendering of the SAF prototype reader showing its key components.

schematic of this optical set-up is given in Fig. 3A. A custom alignment jig (Fig. 3B) allowed precise positioning of the on-disc SAF chips with respect to the excitation and collection optics. The SAF chip (Figs. 1III and 3A) was designed with embedded optics. Details of SAF measurements and characterization can be found in the literature [10,23]. Briefly, surface bound fluorescence dye molecules are excited by the laser diode with a beam diameter of  $\sim 400 \mu\text{m}$ . In a confocal optical setup, an ellipsoidal mirror (Optiforms, USA) is used for collection of SAF emission (light which is at an angle above  $61.5^\circ$ ), which is detected by the photodetector.

### 3.4. Bioprocess monitoring immunoassay for human IgG

We have previously described a fluorescence-linked immunosorbent assay (FLISA) using conventional instrumentation for the detection of human-IgG (hIgG) [15]. In this study, we have modified and applied this hIgG FLISA for use in a SAF-based centrifugal microfluidic system. Prior to microfluidic FLISA testing, reagents were diluted with phosphate buffer saline (PBS, 150 mM, pH 7.4) and Tween<sup>®</sup> 20 (TW-20) (PBST). In addition, a biotinylated, secondary anti-human-IgG antibody (Ab) (Gallus Immunotech Inc., USA) and a biotin-binding fluorescent protein conjugate, Neutravidin-Dylight 650 (Dy) (Piercenet, USA) were diluted in PBST at a ratio of 3:1. This fluorescence detection reagent (AbDy) was subsequently incubated in the dark at  $37^\circ\text{C}$  for 20 min. FLISA reagents ( $30 \mu\text{L}$ ) were added into their designated chambers, and propelled across the protein A capture spot (Fig. 1III and IV).

The delivery sequence and TW-20 concentrations of the FLISA reagents were as follows: BSA (1%, w/v, in PBST with 0.6%, v/v, TW-20), hIgG standards (0.16, 0.8, 2, 4, 20, 50,  $100 \mu\text{g mL}^{-1}$ ) and diluted bioprocess sample (PBST with 0.6%, v/v, TW-20), wash solution 1 (PBST with 0.4%, v/v, TW-20), AbDy (PBST with 0.7%, v/v, TW-20) and wash solution 2 (PBST with 0.4%, v/v, TW-20). The bioprocess sample was supplied by EMD Millipore Corporation. Fluorescence measurements were taken after the last wash step using our prototype SAF reader system. The excitation and emission wavelengths were 635 nm and 676 nm, respectively. It should be noted that the concentration of TW-20 in each of the FLISA reagents was significantly optimized, so as to facilitate the function of the siphon valves. This study is detailed in Section 4.1 below.

## 4. Results and discussion

This work describes the application of an integrated immunoassay linked to microfluidic technology for application in bioprocess monitoring. For the first time, SAF optical detection has been automated and integrated with a centrifugal microfluidic platform, to enable surface-specific fluorescence detection of a heterogeneous immunoassay. Moreover, the SAF optical elements have been incorporated onto the microfluidic disc itself. Plasma technology was used to polymerize APTES onto the surface of the SAF chip to mediate immobilisation of specific capture proteins. A quantitative, surface-based, hIgG immunoassay was developed and used to test this system. The concentration of TW-20 in each of the assay reagents was optimized to facilitate the function of the serial siphon and capillary valves while still maintaining optimal assay functionality. Furthermore, the hardware platform to interface with the integrated microfluidic device was successfully developed.

### 4.1. Optimization of TW-20 for siphon valving

Due to the hydrophobic nature of the PMMA substrate (water contact angle  $\sim 60^\circ$ ), and the increased surface roughness from precision milling of the channels, priming of the siphon channels was extremely difficult. In previous work [13], the polymer and adhesive layers of the disc platform were

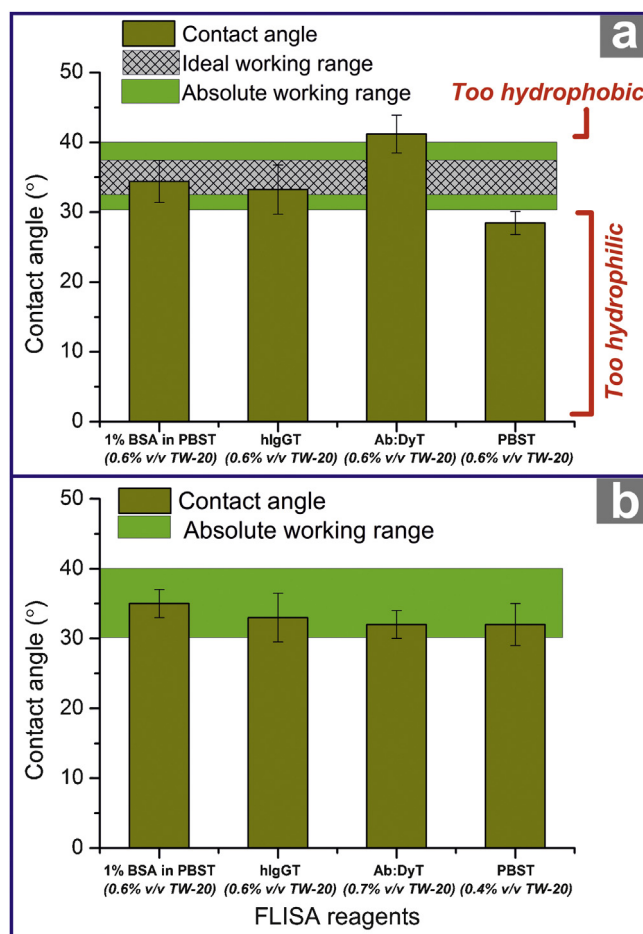


**Fig. 4.** Optimization of the microfluidic immunoassay conditions by varying TW-20 concentration in the FLISA reagents a) contact angle measurements of similar concentration of TW-20 in the four FLISA reagents on untreated PMMA substrate, and b) contact angle measurements of the different optimized concentrations of TW-20 in the reagents on untreated PMMA substrates. The ideal working range corresponds to the preferred contact angle for proper functioning of the siphons, while the absolute working range is the upper and lower limits, outside of which the siphons will not operate at all.

plasma-treated before assembly in order to facilitate priming of the siphon channels. However, hydrophobic recovery of plasma treated polymer substrates is well documented in the literature [29,30], making this technique highly unreliable.

It was hypothesized that the addition of a surfactant [31,32] (TW-20) to the assay reagents would reduce their surface tension, thus making it easier to prime the siphon channels. Titration studies of the immunoassay reagents and TW-20 concentrations were carried out in order to determine the minimal TW-20 concentration, which would facilitate sequential delivery of the FLISA reagents. Fig. 4 demonstrates that it was critical to individually optimise TW-20 concentration for each FLISA reagent.

When 0.6%, v/v, TW-20 was added to all assay reagents, their contact angles (CA) when measured on a plain PMMA substrate varied (Fig. 4a). Subsequently, these assay reagents were tested in the serial siphon channels. The 1%, w/v, BSA (CA =  $34^\circ$ ) and hIgG (CA =  $33^\circ$ ) solutions satisfactorily primed the siphon channels. However, the PBS (CA =  $28^\circ$ ) solution primed the siphon channels uncontrollably, whereas, the AbDy (CA =  $41^\circ$ ) reagent was unable to prime the siphon channel. Therefore, following a series of empirical optimisations, the range for the ideal and absolute working contact angles were determined (Fig. 4b).

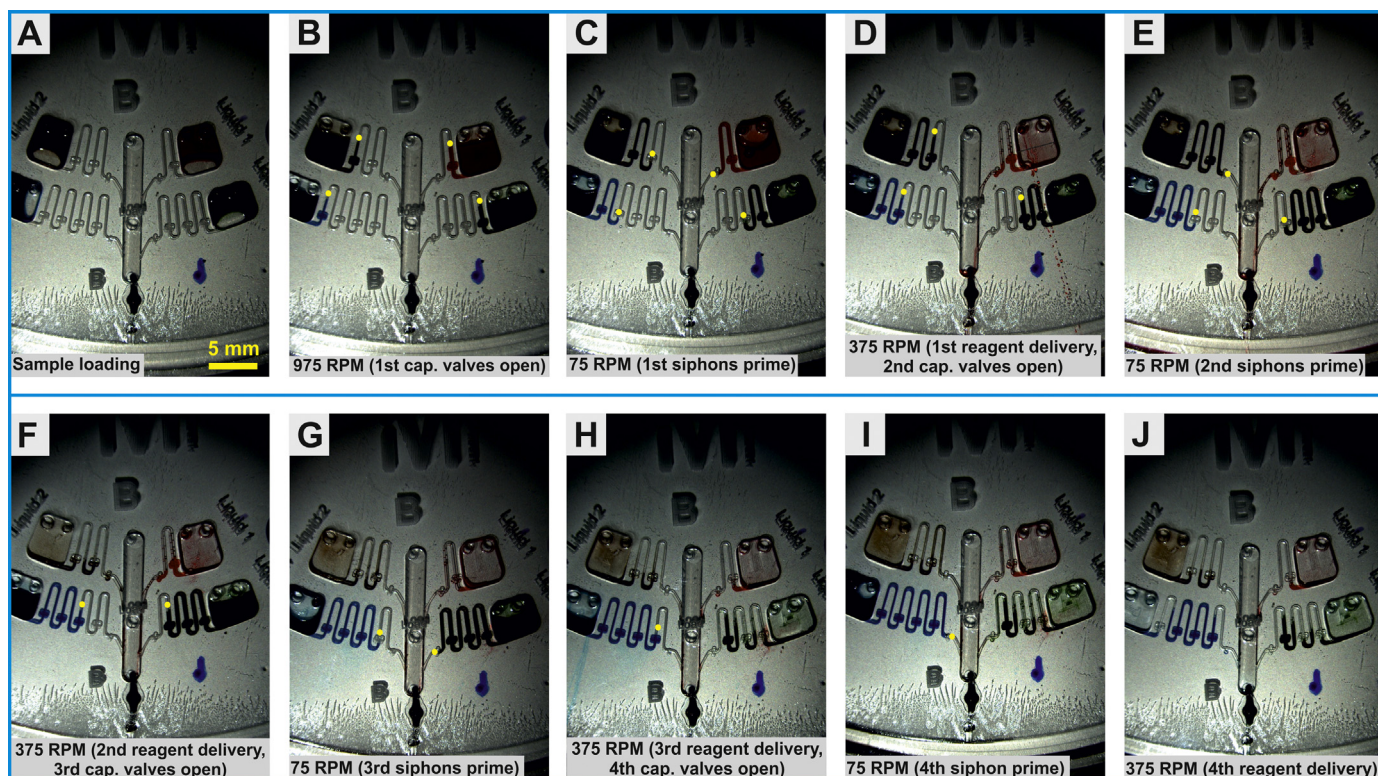


**Fig. 5.** Frame sequence of the serial siphons interspersed by inline capillary valves showing the sequential delivery of four reagents over the sensor spot. The yellow spots in the images indicate key functional locations at different times and spin speeds. (A) At high spinning frequencies  $\sim 975$  RPM, the capillary valves burst; and the centrifugal force holds back the liquid in the siphon channels. (B) At low frequencies  $\sim 75$  RPM, liquid reagent primes the siphon channel by capillary action, and stops at the next inline capillary valve. (C) At  $\sim 375$  RPM, liquid reagent is delivered to the sensor spot. This spin protocol is repeated (D–J) to sequentially deliver all four reagents to the sensor spot (see also Fig. 2).

The ideal working range ( $33^\circ$ – $37^\circ$ ) is the preferred contact angle, whilst the absolute working range ( $30^\circ$ – $40^\circ$ ) constitutes the limit of the upper and the lower contact angle, outside which the siphons do not function reliably. For example, they are either very hydrophobic (reagent does not prime the siphons) or very hydrophilic (reagent primes the siphons uncontrollably, such that the inline capillary valves are unable to function properly). Therefore, prior to testing the microfluidic platform, the contact angle of the reagents was measured to ensure that they were within the absolute working range.

In this work, addition of TW-20 to the FLISA reagents was sufficient to reliably prime the siphons and burst the in-line capillary valves; however, this technique may not be ideal for large scale commercial application. Work is currently on-going to develop a more robust hydrophilization method of the substrate surface suitable for this application, for example siloxane coating [33].

#### 4.2. Serial siphon valving

Although the concept of serial siphoning on centrifugal microfluidic platforms was previously reported [13], this valving scheme has never been used to automate the controlled, sequential release of multiple reagents in a heterogeneous, flow-based immunoassay (Fig. 5).

To characterize the microfluidic platform and siphon valves, contrast agent ( $<1\%$ , v/v) was added to phosphate buffered saline (PBS, 150 mM, pH 7.4) and loaded onto the disc. Aliquots (30- $\mu$ L) that included the (mock) sample, wash 1, fluorescent label, and wash 2 were first manually pipetted onto the disc. The appropriate spin protocol was then initiated, consisting of four consecutive repeats of  $\sim 975$  revolutions-per-minute (RPM) to burst the inline capillary valves ( $<30$  s), followed by 30 s at  $\sim 75$  RPM to prime the

siphon(s) via capillary action, and a final 4 min at  $\sim 375$  RPM to flow the reagent across the active assay area on the SAF chip (Fig. 2B). An incubation step of 2 min was observed in-between each assay reagent flowing over the active assay spot. The design of the serial siphons, inline capillary valves and the spin profile were specifically optimized for this application. Visualization and monitoring of the on-disc fluidics was achieved using a servo-motor coupled to a stroboscope imaging system, similar to systems previously reported in the literature [28].

The entire siphon valving sequence for all reagents was completed in less than 30 min, without the need for operator intervention<sup>2</sup> (see also Fig. 2B). A full video of the sequential reagent delivery of the assay reagents can be found in the *ESI*<sup>1</sup>.

Overall, the serial siphons proved their ability to provide adequate flow control capability for the liquid handling required for implementing the hIgG assay.

#### 4.3. Quantification of the integrated hIgG immunoassay

A standard curve for a hIgG immunoassay was successfully demonstrated using centrifugal microfluidics and a SAF prototype detector. In total seven hIgG standards, a bioprocess sample and a blank sample were measured in triplicate using the integrated serial siphon SAF disc and the SAF reader hardware. Analysis was performed on two different days. Fig. 6B shows an inter-day hIgG

<sup>2</sup> Only during the later stages of the assay optimization it was realized that a fifth reagent (PBST wash) further improved assay performance. As we needed to use the existing batch of disc replicates, this reagent was loaded manually through the central channel (Fig. 1II). However, it is evident that this step may readily be automated by another reservoir connected through an additional siphon (winding) to the common flow channel.

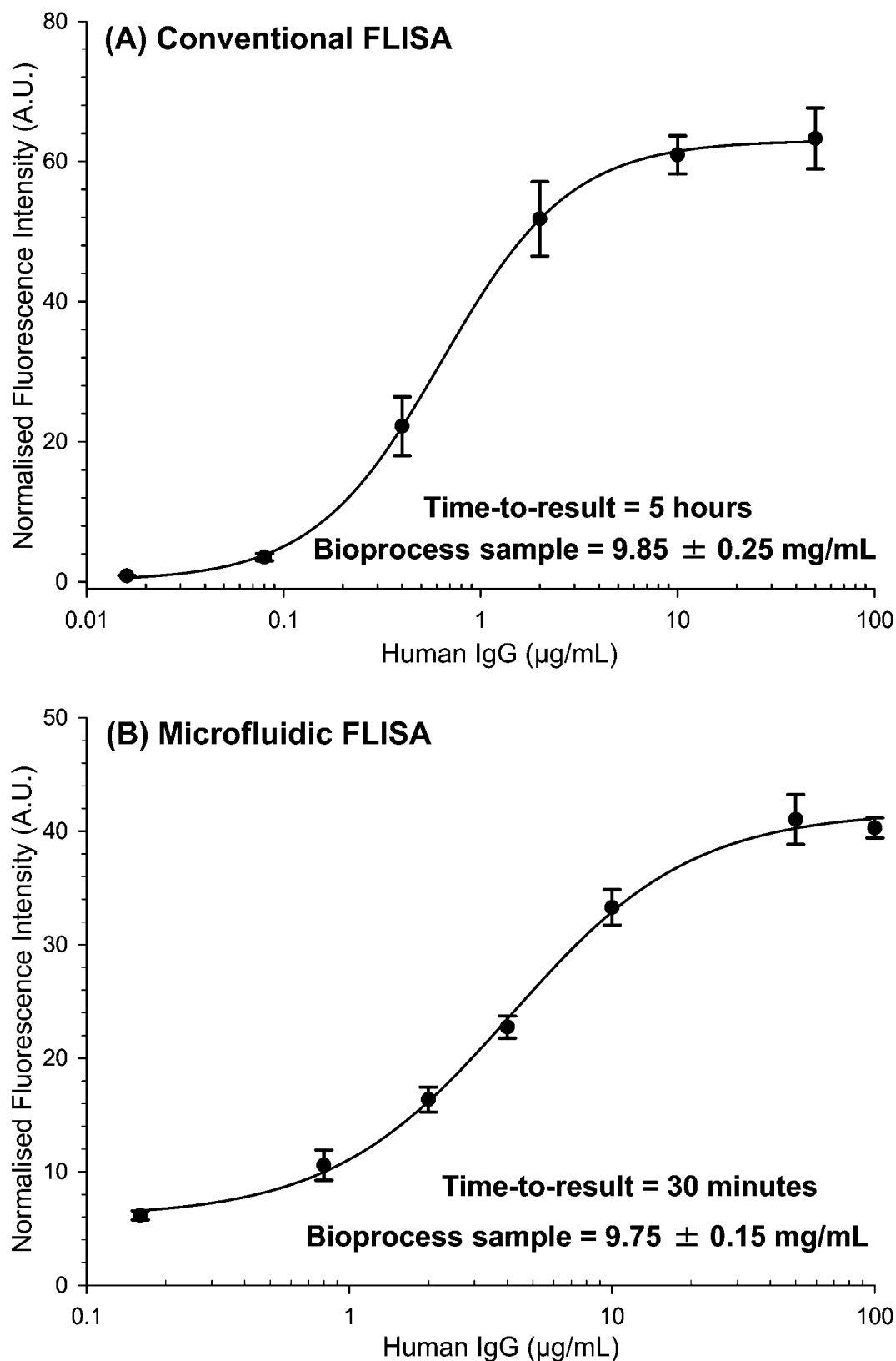


**Fig. 6.** hIgG FLISA calibration curves. (A) Conventional FLISA performed with high protein binding well plates and a commercial fluorescent detector. (B) Microfluidic FLISA performed with an experimental PECVD APTES-treated Zeonor<sup>®</sup> surface, microfluidic serial siphon valving system and a prototype SAF detector (Fig. 3B).

calibration curve exhibiting a coefficient of variation (CV) of 2.2% to 12.6% across the entire hIgG concentration range, on the microfluidic platform. In contrast, the conventional FLISA (Fig. 6A) displayed greater imprecision as the within-day CV range was 5.9% to 18.9%.

Calibration curves from both analyses were used to quantify a typical bioprocess sample which had a hIgG concentration of  $\sim 10 \text{ mg mL}^{-1}$ . Prior to analysis, the bioprocess sample was diluted in PBST. There was good agreement between both

methods as conventional FLISA analysis yielded a hIgG concentration of 9.6–10.1 mg mL<sup>-1</sup>, whereas, the serial siphon-based centrifugal microfluidic platform yielded a hIgG concentration range of 9.6–9.9 mg mL<sup>-1</sup>. However, a comparison of both standard curves revealed a shift in the range of the hIgG assay. The dynamic ranges were ~0.08–10 µg mL<sup>-1</sup> for the conventional FLISA, and ~0.8–50 µg mL<sup>-1</sup> for the microfluidic FLISA. The smaller range of the microfluidic FLISA was somewhat expected as our device is a prototype system that contains not only an experimental protein capture surface but also experimental signal detection and reagent delivery systems. In contrast, conventional hIgG FLISA analysis was carried out with standard microtitre plates that have excellent protein binding properties as well as low autofluorescence levels. In addition, a commercially available microplate reader with high fluorescent sensitivity was used for sample analysis. Further optimisation of the microfluidic design, surface chemistry and the fluorescence detector has the potential to yield a lower hIgG working range for the SAF-based microfluidic method. However, for our particular application the target analyte is in relative abundance. For example, bioprocess samples typically contain milligram amounts of hIgG per millilitre [34]. Therefore, the shift in assay range was desirable, as it reduced the dilution needed to allow the sample to fall within the linear range of the calibration curve. In addition, a preliminary shelf-life assessment of the protein A surface was performed. IgG–FLISA analysis on a microfluidic chip revealed no significant differences in fluorescence intensity between zero-day-old and one-month-old chips. More detailed results of this protein A stability study can be found in the *ESI*<sup>1</sup>.

#### 4.4. SAF measurements and custom benchtop instrument

As the laser beam of the SAF detector was only ~400 µm in diameter, it was necessary to provide a homogeneous fluorescence assay spot. To minimise the overall assay error, a significant amount of time was invested in optimizing APTES surface functionalization of the SAF lens, concentration of the biomolecule capture reagent coating, assay incubation steps and laser alignment of the SAF detector. The SAF prototype reader was fabricated out of relatively inexpensive parts (~€1500) yet it performs similarly to conventional, but more expensive instrumentation.

In its current form (*inset* Fig. 3A), the instrument is compact and amenable to transport around the production floor of a pharmaceutical manufacturer. The centrifugal sub-assembly provided the required speeds for microfluidic pumping with desirable acceleration, deceleration, and control characteristics. The optical SAF system enabled quantitation of the hIgG immunoassay. A custom alignment jig, developed to help enhance optical positioning of the microfluidic platform and the SAF instrument drastically reduced inconsistencies in the SAF measurements. A low optical noise background was provided by a light-proof dark casing for sensitive SAF detection. For fluorescence detection, raw fluorescence intensity data were collected using the LabVIEW program (3 independent measurements on each SAF chip, with each measurement  $n=20$ ) and then analysed and processed using a customized Excel macro. In total, the seven hIgG samples and the bioprocess sample were tested in triplicate.

## 5. Conclusions and outlook

Our prototype system represents a key step forward towards the development of a commercial, at-line, sample-to-answer, protein monitoring tool for the bioprocess industry. A surface-based immunoassay for monitoring hIgG in a bioprocess workflow was successfully demonstrated using a serial siphon valving scheme for automated reagent delivery. It was shown that that plasma

polymerized APTES deposited on the surface of the SAF lens facilitated the homogeneous immobilization of the biomolecular capture proteins. The prototype SAF hardware system was used to determine the hIgG concentration of an industrial bioprocess sample.

Development is underway to program the SAF prototype reader for full automation of all processes and also for the detection of analytes at very low concentrations. Future steps include incorporation of the bioprocess sample preparative steps (*viz.*, removal of cells and sample dilution series) on our lab-on-a-disc platform.

## Acknowledgements

This work was supported by the Science Foundation Ireland (Grant Nos. 05/CE3/B754, 05/CE3/B754S6 and 10/CE/B1821).

## Appendix A. Supplementary data

Supplementary data associated with this article can be found, in the online version, at <http://dx.doi.org/10.1016/j.aca.2013.04.016>.

## References

- [1] M. Miró, E.H. Hansen, Miniaturization of environmental chemical assays in flowing systems: The lab-on-a-valve approach vis-a-vis lab-on-a-chip microfluidic devices, *Anal. Chim. Acta* 600 (2007) 46–57.
- [2] R. Gorkin, J. Park, J. Siegrist, M. Amasia, B.S. Lee, J.M. Park, J. Kim, H. Kim, M. Madou, Y.K. Cho, Centrifugal microfluidics for biomedical applications, *Lab Chip* 10 (2010) 1758–1773.
- [3] D. Erickson, D. Li, Integrated microfluidic devices, *Anal. Chim. Acta* 507 (2004) 11–26.
- [4] H. Kido, A. Maquieira, B.D. Hammock, Disc-based immunoassay microarrays, *Anal. Chim. Acta* 411 (2000) 1–11.
- [5] D. Pioch, B. Jürgen, S. Evers, K.H. Maurer, M. Hecker, T. Schweder, At-line monitoring of bioprocess-relevant marker genes, *Eng. Life Sci.* 7 (2007) 373–379.
- [6] H.L.T. Lee, P. Boccazzi, N. Gorret, R.J. Ram, A.J. Sinskey, In situ bioprocess monitoring of *Escherichia coli* bioreactions using Raman spectroscopy, *Vib. Spectrosc.* 35 (2004) 131–137.
- [7] C.-F. Mandenius, Recent developments in the monitoring, modeling and control of biological production systems, *Bioprocess. Biosyst. Eng.* 26 (2004) 347–351.
- [8] J.D. Moore, M.A. Perez-Pardo, J.F. Popplewell, S.J. Spencer, S. Ray, M.J. Swann, A.G. Shard, W. Jones, A. Hills, D.G. Bracewell, Chemical and biological characterisation of a sensor surface for bioprocess monitoring, *Biosens. Bioelectron.* 26 (2011) 2940–2947.
- [9] M. Akin, A. Prediger, M. Yuksel, T. Höpfner, D.O. Demirkol, S. Beutel, S. Timur, T. Scheper, A new set up for multi-analyte sensing: At-line bio-process monitoring, *Biosens. Bioelectron.* 26 (2011) 4532–4537.
- [10] D. Kurzbuch, J. Bakker, J. Melin, C. Jönsson, T. Ruckstuhl, B.D. MacCraith, A biochip reader using super critical angle fluorescence, *Sensor Actuat. B - Chem.* 137 (2009) 1–6.
- [11] B. Kuswandi, Nuriman, J. Huskens, W. Verboom, Optical sensing systems for microfluidic devices: a review, *Anal. Chim. Acta* 601 (2007) 141–155.
- [12] L. Novak, P. Neuzil, J. Pipper, Y. Zhang, S. Lee, An integrated fluorescence detection system for lab-on-a-chip applications, *Lab Chip* 7 (2007) 27–29.
- [13] J. Siegrist, R. Gorkin, L. Clime, E. Roy, R. Peytavi, H. Kido, M. Bergeron, T. Veres, M. Madou, Serial siphon valving for centrifugal microfluidic platforms, *Microfluid. Nanofluid.* 9 (2010) 55–63.
- [14] V. Gubala, R.P. Gandhiraman, C. Volcke, C. Doyle, C. Coyle, B. James, S. Daniels, D.E. Williams, Functionalization of cycloolefin polymer surfaces by plasma-enhanced chemical vapour deposition: comprehensive characterization and analysis of the contact surface and the bulk of aminosiloxane coatings, *Analyst* 135 (2010) 1375–1381.
- [15] R. Gorkin III, C.E. Nwankire, J. Gaughran, X. Zhang, G.G. Donohoe, M. Rook, R. O'Kennedy, J. Duce, Centrifugo-pneumatic valving utilizing dissolvable films, *Lab Chip* 12 (2012) 2894–2902.
- [16] R.P. Gandhiraman, C. Volcke, V. Gubala, C. Doyle, L. Basabe-Desmonts, C. Dotzler, M.F. Toney, M. Iacono, R.I. Nooney, S. Daniels, B. James, D.E. Williams, High efficiency amine functionalization of cycloolefin polymer surfaces for biodiagnostics, *J. Mater. Chem.* 20 (2010) 4116–4127.
- [17] J. Duce, S. Haerberle, S. Lutz, S. Pausch, F.V. Stetten, R. Zengerle, The centrifugal microfluidic Bio-Disk platform, *J. Micromech. Microeng.* 17 (2007) S103–S115.
- [18] M. Madou, J. Zoval, J. Guanyao, H. Kido, J. Kim, N. Kim, Lab on a CD, *Annu. Rev. Biomed. Eng.* 8 (2006) 601–628.
- [19] R. Peytavi, F.R. Raymond, D. Gagné, F.J. Picard, G. Jia, J. Zoval, M. Madou, K. Boissinot, M. Boissinot, L. Bissonnette, M. Ouellette, M.G. Bergeron, Microfluidic device for rapid (<15 min) automated microarray hybridization, *Clin. Chem.* 51 (2005) 1836–1844.
- [20] S. Haerberle, R. Zengerle, Microfluidic platforms for lab-on-a-chip applications, *Lab Chip* 7 (2007) 1094–1110.

- [21] N. Godino, R. Gorkin, A.V. Linares, R. Burger, J. Ducreé, Comprehensive integration of homogeneous bioassays via centrifugo-pneumatic cascading, *Lab Chip*. 13 (2013) 685–694.
- [22] J. Steigert, T. Brenner, M. Grumann, L. Riegger, S. Lutz, R. Zengerle, J. Ducreé, Integrated siphon-based metering and sedimentation of whole blood on a hydrophilic lab-on-a-disk, *Biomed. Microdevices* 9 (2007) 675–679.
- [23] D. Kurzbuch, J.W.P., Bakker, T., Ruckstuhl, J. Melin,;1; Super Critical Angle Fluorescence Scanning System, in: U.P.T. Office (Ed.), United States, 2010.
- [24] S. Melamed, L. Ceriotti, W. Weigel, F. Rossi, P. Colpo, S. Belkin, A printed nanolitre-scale bacterial sensor array, *Lab Chip*. 11 (2011) 139–146.
- [25] J. Kim, E.C. Jensen, M. Megens, B. Boser, R.A. Mathies, Integrated microfluidic bioprocessor for solid phase capture immunoassays, *Lab Chip*. 11 (2011) 3106–3112.
- [26] D.A. Bartholomeusz, R.W. Boulté, J.D. Andrade, Xurography rapid prototyping of microstructures using a cutting plotter, *J. Microelectromech. Syst.* 14 (2005) 1364–1374.
- [27] S. Xiang, G. Xing, W. Xue, C. Lu, J.-M. Lin, Comparison of two different deposition methods of 3-aminopropyltriethoxysilane on glass slides and their application in the thinprep cytologic test, *Analyst* 137 (2012) 1669–1673.
- [28] M. Grumann, T. Brenner, C. Beer, R. Zengerle, J. Ducreé, Visualization of flow patterning in high-speed centrifugal microfluidics, *Rev. Sci. Instrum.* 76 (2005), 025101–025101–025106.
- [29] C.E. Nwankire, G. Favaro, Q.-H. Duong, D.P. Dowling, Enhancing the mechanical properties of superhydrophobic atmospheric pressure plasma deposited siloxane coatings, *Plasma Process. Polym.* 8 (2011) 305–315.
- [30] D.P. Dowling, C.E. Nwankire, M. Riihimäki, R. Keiski, U. Nylén, Evaluation of the anti-fouling properties of nm thick atmospheric plasma deposited coatings, *Surf. Coat. Technol.* 205 (2010) 1544–1551.
- [31] A. Gunther, K.F. Jensen, Multiphase microfluidics: from flow characteristics to chemical and materials synthesis, *Lab Chip*. 6 (2006) 1487–1503.
- [32] Y.C. Kim, S.-H. Kim, D. Kim, S.-J. Park, J.-K. Park, Plasma extraction in a capillary-driven microfluidic device using surfactant-added poly(dimethylsiloxane), *Sensor Actuat. B – Chem.* 145 (2010) 861–868.
- [33] V. Gubala, J. Siegrist, R. Monaghan, B. O'Reilly, R.P. Gandhiraman, S. Daniels, D.E. Williams, J. Ducreé, Simple approach to study biomolecule adsorption in polymeric microfluidic channels, *Anal. Chim. Acta* 760 (2013) 75–82.
- [34] T. Scheper, B. Hitzmann, E. Stärk, R. Ulber, R. Faurie, P. Sosnitza, K. Reardon, Bioanalytics: detailed insight into bioprocesses, *Anal. Chim. Acta* 400 (1999) 121–134.